

DRUG SYNTHESIS

SYNTHESIS, PRO-APOPTOTIC ACTIVITY AND 2D-QSAR STUDIES
OF NEW ANALOGUES OF FLUPHENAZINEJOANNA ŻYTA¹, AGATA JASZCZYSZYN^{2*}, PIOTR ŚWIĄTEK³, KAZIMIERZ GAŚSIOROWSKI²
and WIESŁAW MALINKA³¹Faculty of Chemistry, University of Wrocław, Joliot-Curie 14, 50-383 Wrocław, Poland²Department of Basic Medical Sciences, Wrocław Medical University,
Borowska 211, 50-556 Wrocław, Poland³Department of Drug Chemistry, Wrocław Medical University, Borowska 211, 50-556 Wrocław, Poland

Abstract: A series of 10 novel analogues of fluphenazine (FPh) were synthesized. Influence of the synthesized analogues of FPh on frequency of apoptosis and necrosis in cultures of human lymphocytes genotoxically damaged *in vitro* with benzo[*a*]pyrene (B[*a*]P; 7.5 μ M, 48 h) was compared with the effect of FPh. Activity of the tested compounds was expressed by ED₅₀ (pro-apoptotic activity) and TD₅₀ (pro-necrotic effect, cytotoxicity). It was noticed that compounds **3–9** and **12** exerted a pro-apoptotic effect markedly stronger than that of FPh. Additionally, compounds **3**, **9** and **10** exhibited the weakest influence on frequency of necrotic lymphocyte in cultures. 2D-QSAR analysis was done in order to find quantitative relationship between structures of the tested analogues and their pro-apoptotic activity or pro-necrotic effect in B[*a*]P-damaged cell cultures. Several statistically significant QSAR models were generated. Information obtained from 2D-QSAR study will be used in further design of analogues of FPh more active in cancer chemoprevention.

Keywords: fluphenazine analogues, synthesis, pro-apoptotic activity, 2D-QSAR study

Phenothiazine derivatives (Pht), among them also fluphenazine (FPh), exert an anti-psychotic activity by binding and inhibition of an array of presynaptic dopaminergic receptors and for years various drugs from phenothiazine family have been used in psychopharmacotherapy (1). Aside from their neuroleptic activity Pht also possess cancer chemopreventive activity – they inhibit the calmodulin, the protein kinase C, and decrease the transporter function of P-glycoprotein (2, 3). Importantly, recent papers documented an anti-cancer activity of various Pht in cultures of human cancer cell lines (4, 5). Randomized prospective trials of patients with schizophrenia, treated with phenothiazines found that the occurrence rate of cancer was smaller than in healthy people from the control group (6). The mechanism of cancer prevention by Pht is weakly known. However, some experimental results showed that various phenothiazine compounds are able to induce *in vitro* a programmed cell death (apoptosis) in tumor cells and/or in genotoxically damaged cells (7, 8). It is broadly accepted that

a stimulation of apoptosis in cancer cells could be an important mechanism of action of cancer chemopreventive drugs, and it is reasonable that a pro-apoptotic activity should prevail against a cytotoxic activity in the activity profile requested for those drugs (9, 10).

Pht have been used for years in the treatment of patients with schizophrenia, and recently they are also assayed for anti-mutagenic and anti-cancer activities (11). It was estimated that Pht exhibited strong pro-apoptotic activity *in vitro* (10, 12). However, their usefulness in cancer therapy in humans is limited by the serious adverse effects on the central nervous system, mainly the extrapyramidal symptoms and induction of the iatrogenic parkinsonism (13). The FPh analogues, synthesized by us, possess several structural modification of the side chain, lower value of log of the octanol/water partition coefficient or higher molecular weight than the parent compound. Therefore, we suggest that their penetration through blood-brain barrier into the central nervous system should be markedly weaker

* Corresponding author: e-mail: agata.jaszczyszyn@am.wroc.pl

and extrapyramidal side effects will be decreased in comparison with FPh.

In the present study, 10 novel analogues of FPh were synthesized and evaluated for their pro-apoptotic activity and pro-necrotic effect (cytotoxicity) in cultures of human lymphocytes genotoxically damaged *in vitro* by incubation with benzo[*a*]pyrene (B[*a*]P; 7.5 μ M, 48 h). 2D-QSAR analysis was done in order to find quantitative relationship between structures of the tested compounds and their pro-apoptotic activity or pro-necrotic effect in B[*a*]P-damaged cell cultures. Information obtained from 2D-QSAR study will be used in further design of FPh analogues more active in cancer chemoprevention.

EXPERIMENTAL

Chemistry

Melting points are uncorrected. ¹H NMR spectra were recorded in CDCl₃ at 80 MHz using a Tesla spectrometer or at 300 MHz using a Bruker spectrometer. ¹H chemical shifts were reported in δ (ppm). Elemental analyses were within \pm 0.4% of the theoretical values and were performed on a Carlo Erba NA-1500 analyzer. All reactions were monitored by thin-layer chromatography on 0.25 mm Merck silica gel (60 F₂₅₄) and visualized by UV light (λ = 264 or 365 nm). Flash chromatography was performed on a silica gel Kieselgel 60 (70–230 mesh) Merck.

10-(2,3-Epoxypropyl)-2-trifluoromethylphenothiazine (2)

To a stirred solution of 1.335 g (0.005 mol) of 2-trifluoromethylphenothiazine **1** in 5 mL of dimethylformamide 0.4 g (0.01 mol) of sodium hydride (60% dispersion in mineral oil) was added and the stirring was continued at room temperature for 1 h. Then, 0.85 mL (0.01 mol) of 1-bromo-2,3-epoxypropane was added and the stirring was continued for 3 h. Afterwards, the mixture was diluted with ice-cold water. The liberated in form of dark oil crude product was purified through flash chromatography (cyclohexane/toluene 1 : 1, v/v, R_f = 0.34). The epoxide **2** was obtained in 43% yield.

Formula: C₁₆H₁₂F₃NOS; m.w.: 323.33, m.p. 66–67°C; ¹H NMR (δ , ppm): 2.73–2.99 (m, 2H, CH₂), 3.22–3.39 (m, 1H, CH), 3.71–4.38 (m, 2H, N₁₀-CH₂), 6.92–7.24 (m, 7H, PhtH)

General procedure for preparation of analogues 3–11

A solution of 0.4 g (0.00124 mol) of epoxide **2** and 0.00124 mol of an appropriate amine in 10 mL of

ethanol was refluxed under stirring for 4–18 h. Then, the solvent was evaporated under reduced pressure and the residue was purified through flash chromatography. The obtained products **3–11** were in next step transformed to the corresponding salts by means of ethanol saturated with gas hydrogen chloride.

10-{3-[N,N-bis-(2-hydroxyethyl)amino]-2-hydroxypropyl}-2-trifluoromethylphenothiazine hydrochloride (3)

Formula: C₂₀H₂₄ClF₃N₂O₃S; m.w.: 464.93; m.p.: 192–194°C; 55.5% yield; chromatography: (ethyl acetate/methanol 3 : 1, v/v, R_f = 0.45); ¹H NMR (δ , ppm): 3.23–3.41 (m, 6H, N(CH₂)₃), 3.70–4.51 (m, 7H, N₁₀-CH₂CH and 2CH₂OH), 5.17 (brs, 2H, 2CH₂OH^{ex}), 5.84 (brs, 1H, CHO^{ex}), 6.85–7.30 (m, 7H, PhtH), 7.83 (brs, 1H, N⁺H^{ex}).

S(+)-10-[3-(1-ethyl-2-hydroxyethylamino)-2-hydroxypropyl]-2-trifluoromethylphenothiazine hydrochloride (4)

Formula: C₂₀H₂₄ClF₃N₂O₂S; m.w.: 448.93; m.p.: 187–189°C; 27% yield; chromatography: (ethyl acetate/methanol 5 : 1, v/v, R_f = 0.47); ¹H NMR (δ , ppm): 0.81–0.89 (m, 3H, CH₃), 1.54–1.64 (m, 2H, CH₂CH₃), 2.93–3.12 (m, 2H, CH₂N), 3.46–3.63 (m, 1H, CH), 3.73–3.80 (m, 2H, CH₂OH), 4.17–4.25 (m, 3H, N₁₀-CH₂CH), 4.94 (brs, 1H, CH₂OH^{ex}), 5.74 (brs, 1H, CHO^{ex}), 6.95–7.06 (m, 2H, PhtH), 7.14–7.28 (m, 5H, PhtH), 7.45 (brs, 1H, N⁺H^{ex}), 8.69 (brs, 1H, NH^{ex}).

10-[3-(2,3-Dihydroxypropylamino)-2-hydroxypropyl]-2-trifluoromethylphenothiazine hydrochloride (5)

Formula: C₁₉H₂₂ClF₃N₂O₃S; m.w.: 450.90; m.p.: 56–58°C; 42% yield; chromatography: (ethyl acetate/methanol 1.5 : 1, v/v, R_f = 0.42); ¹H NMR (δ , ppm): 2.80–3.06 (m, 4H, CH₂NCH₂), 3.40–3.46 (m, 2H, CH₂OH), 3.90–4.02 (m, 2H, N₁₀-CH₂), 4.12–4.14 (m, 1H, CH), 4.40–4.44 (m, 1H, CH), 6.89–7.01 (m, 2H, PhtH), 7.08–7.22 (m, 5H, PhtH), 8.16 (brs, 1H, NH).

10-[3-(Morpholin-4-yl)-2-hydroxypropyl]-2-trifluoromethylphenothiazine hydrochloride (6)

Formula: C₂₀H₂₂ClF₃N₂O₂S; m.w.: 446.91; m.p.: 138–140°C; 10.5% yield; chromatography: (ethyl acetate/methanol 4 : 1, v/v, R_f = 0.80); ¹H NMR (δ , ppm): 2.97–3.03 (m, 6H, 3NCH₂), 3.89–3.98 (m, 4H, CH₂OCH₂), 4.21–4.31 (m, 3H, N₁₀-CH₂CH), 5.59 (brs, 1H, CHO^{ex}), 6.99–7.08 (m, 2H, PhtH), 7.16–7.31 (m, 5H, PhtH), 12.23 (brs, 1H, NH^{ex}).

10-{3-[4-(2-Hydroxyethyl)piperazin-1-yl]-2-hydroxypropyl}-2-trifluoromethylphenothiazine dihydrochloride (7)

Formula: $C_{22}H_{28}Cl_2F_3N_3O_2S$; m.w.: 526.42; m.p.: 88–90°C; 48.6% yield; chromatography: (ethyl acetate/methanol 4 : 1, v/v, $R_f = 0.26$); 1H NMR (δ , ppm): 2.39–2.62 (m, 12H, $CH_2N(CH_2CH_2)_2NCH_2$), 3.56–3.61 (m, 2H, CH_2OH), 3.93–4.14 (m, 3H, $N_{10}-CH_2CH$), 4.76 (brs, 1H, CH_2OH^{ex}), 6.94–7.02 (m, 2H, PhtH), 7.14–7.24 (m, 5H, PhtH).

10-{3-[4-(2-Furoil)piperazin-1-yl]-2-hydroxypropyl}-2-trifluoromethylphenothiazine dihydrochloride (8)

Formula: $C_{25}H_{26}Cl_2F_3N_3O_3S$; m.w.: 576.46; m.p.: 140–142°C; 46.5% yield; chromatography: (ethyl acetate, $R_f = 0.62$); 1H NMR (δ , ppm): 2.42–2.64 [m, 6H, $CH_2N(CH_2)_2$], 3.68–3.81 [m, 4H, $N(CH_2)_2$], 4.00–4.11 (m, 3H, $N_{10}-CH_2CH$), 6.37–6.46 (m, 1H, C_5-H), 6.86–7.38 (m, 9H, 7PhtH and $C_{3,4}-H$)

10-{3-[4-(N-isopropylcarbamoylmethyl)piperazin-1-yl]-2-hydroxypropyl}-2-trifluoromethylphenothiazine dihydrochloride (9)

Formula: $C_{25}H_{33}Cl_2F_3N_4O_2S$; m.w.: 581.50; m.p.: 73–75°C; 47% yield; chromatography: (ethyl acetate/methanol 5 : 1, v/v, $R_f = 0.61$); 1H NMR (δ , ppm): 1.14 (d, 6H, $2 \times CH_3$, $J = 2.5$ Hz), 2.51 (s, 10H, $CH_2N(CH_2CH_2)_2N$), 2.94 (s, 2H, NCH_2CO), 3.91–4.21 (m, 4H, $N_{10}-CH_2CH$ and CH_3CHCH_3), 4.55–4.63 (brs, 1H, NH^{ex}), 6.86–7.33 (m, 7H, PhtH).

10-{3-[4-(4-Acetyl-4-phenyl)piperidin-1-yl]-2-hydroxypropyl}-2-trifluoromethylphenothiazine hydrochloride (10)

Formula: $C_{29}H_{30}ClF_3N_2O_2S$; m.w.: 563.11; m.p.: 113–115°C; 49% yield; chromatography: (ethyl acetate, $R_f = 0.60$); 1H NMR (δ , ppm): 1.88 (s, 3H, CH_3), 2.18–2.66 (m, 10H, $CH_2N(CH_2CH_2)_2$), 3.90–4.16 (m, 3H, $N_{10}-CH_2CH$), 6.93–7.32 (m, 12H, 7PhtH and 5ArH).

10-{3-(3-N,N-diethylcarbamoyl)piperidin-1-yl}-2-hydroxypropyl}-2-trifluoromethylphenothiazine hydrochloride (11)

Formula: $C_{26}H_{33}ClF_3N_3O_2S$; m.w.: 544.07; m.p.: 114–116°C; 43% yield; chromatography: (ethyl acetate/methanol 4 : 1, v/v, $R_f = 0.46$); 1H NMR (δ , ppm): 1.02 (t, $J = 7.2$ Hz, 3H, CH_3), 1.19 (t, $J = 7.2$ Hz, 3H, CH_3), 2.18–2.44 (m, 4H, $NCH_2CH_2CH_2$), 2.62–2.76 (m, 2H, NCH_2CH_2), 2.95–3.05 (m, 2H, NCH_2CH_2), 3.22–3.37 (m, 4H,

$CH_3CH_2NCH_2CH_3$), 3.46–3.56 (m, 2H, $CHCH_2N$), 3.80–3.88 (m, 2H, $N_{10}-CH_2$), 4.22–4.30 (m, 1H, $CHOH$), 4.51–4.64 (m, 1H, CH_2CHCH_3), 6.96–7.04 (m, 2H, PhtH), 7.12–7.32 (m, 5H, PhtH), 11.52 (brs, 1H, N^+H).

10-{4-[4-(2-Pyrimidinyl)piperazin-1-yl]-butyl}-2-trifluoromethylphenothiazine dihydrochloride (12)

A mixture of 1.34 g (0.005 mol) of 2-trifluoromethylphenothiazine **1**, 2.24 g (0.0075 mol) of 8-(2-pyrimidinyl)-8-aza-5-azaspiro[4,5]decane bromide and 1.04 g (0.0075 mol) of anhydrous K_2CO_3 in 30 mL of xylene was stirred and heated under reflux for 20 h. The hot reaction mixture was filtered and the filtrate was concentrated *in vacuo*. The residue was purified through flash chromatography (ethyl acetate/hexane 3 : 1, v/v, $R_f = 0.44$). The free base was converted to the hydrochloride salt **12**.

Formula: $C_{25}H_{28}Cl_2F_3N_5S$; m.w.: 558.57; m.p.: 78–80°C; 10% yield; 1H NMR (δ , ppm): 1.72–2.04 (m, 4H, $-CH_2CH_2-$), 2.30–2.57 (m, 6H, $-CH_2N(CH_2)_2$), 3.74–3.85 (m, 4H, $N(CH_2)_2$), 3.95–4.12 (m, 2H, $N_{10}-CH_2$), 6.38–6.47 (m, 1H, $H_{5-pyrimidine}$), 6.82–7.18 (m, 7H, PhtH), 8.25 (s, 1H, $H_{pyrimidine}$), 8.28 (s, 1H, $H_{pyrimidine}$).

Biological activity

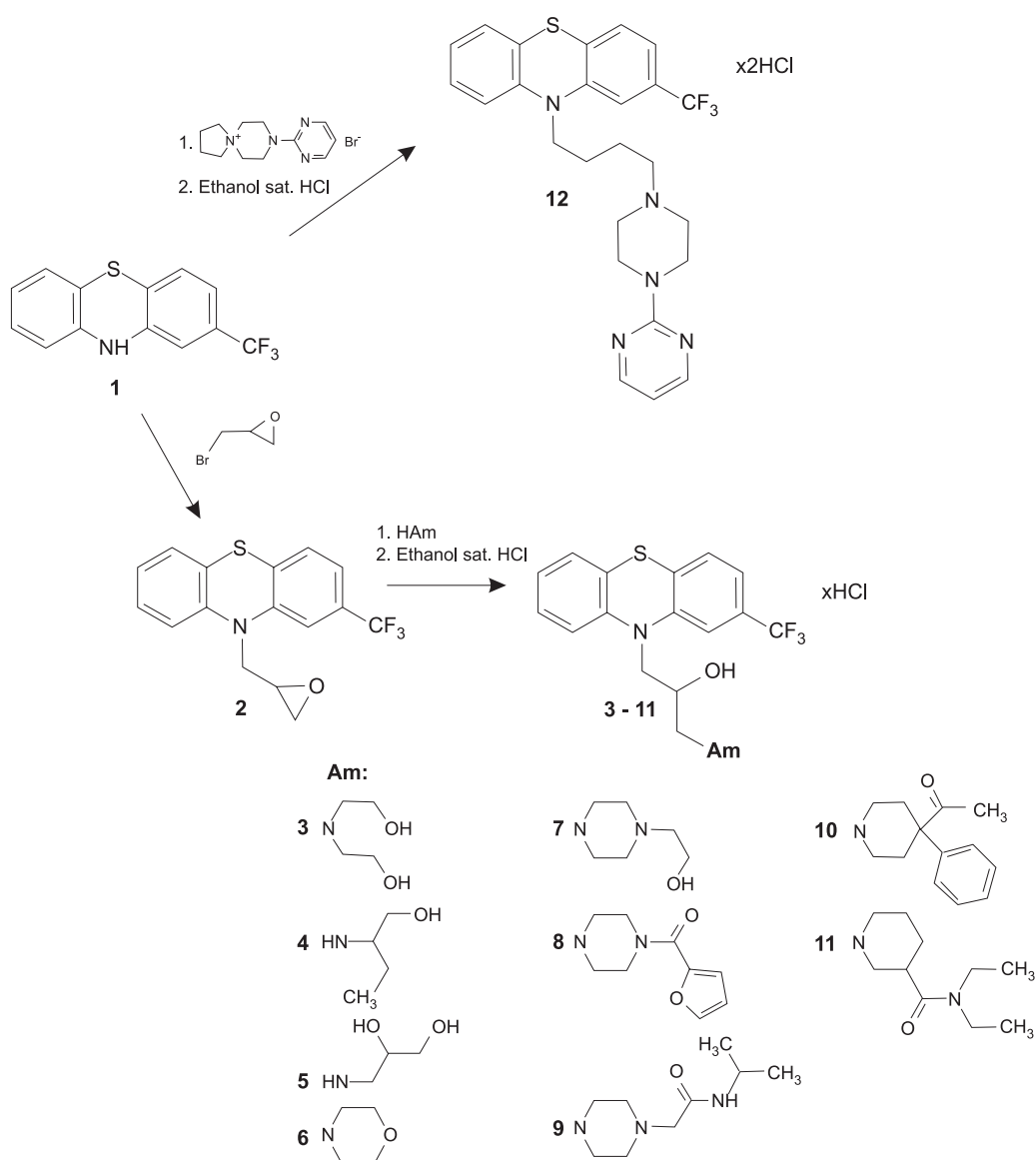
Lymphocytes were isolated from venous blood obtained from five healthy male donors aged 20–26. Cells were separated by the standard technique of blood centrifugation with Histopaque-1077 (Sigma, MO, USA) (14). Lymphocytes were counted and cultured for 48 h in the presence of lectin PHA-M (2% v/v) and the standard genotoxic agent - B[a]P (7.5 μ M, 37°C). The tested compounds: FPh or its chemical analogues, were added to the cultures for 2 h. At the end of a culture time cells were centrifuged, diluted with buffered salt solution (PBS) and stained with fluorochrome mixture - the Annexin V-FITC/propidium iodide staining kit (Sigma, MO, USA) (14). Smears of the stained cell suspensions were examined under a fluorescence microscope, and frequency of necrotic (red fluorescence), apoptotic (green fluorescence) and viable cells (non-stained) were scored among 500 cells randomly found under the microscope image. The effect of 10 analogues of FPh on frequency of apoptosis (A) and necrosis (N) in genotoxicity damaged cell cultures were expressed in proportion to the appropriate reference culture (A_o or N_o). The reference lymphocyte cultures were genotoxicity damaged with B[a]P and incubated with the FPh. The biological activity of the tested compounds was

expressed by (pro-apoptotic activity) ED_{50} and (pro-necrotic effect, cytotoxicity) TD_{50} and showed as A/N index.

Computational details

Molecular structures of all 10 new synthesized compounds were optimized using DFT (Density Functional Theory) method with the B3LYP hybrid exchange-correlation energy functional and 6-31g* basis set (Gaussian03 software package) (15). Because the basic tertiary nitrogen atom in the

aliphatic chain could to be highly protonated at physiological pH – both the neutral and monoprotonated forms were analyzed (16). Initial molecules were built in GaussView program based on the crystal structure of trifluoperazine hydrochloride, which was found in literature data (17). In QSAR investigation, a three-dimensional structure of the compounds inevitably is a key parameter (18, 19). This parameter is crucial in interaction between potential drug and its biological target (20, 21). To obtain the low-energy conformations of new FPh analogues we



Scheme 1. Synthesis of new analogues of FPh

performed conformational analysis of all compounds using one of the semi-empirical methods – Austin Model 1 (AM1). In succeeded investigation we used only the conformation with the lowest energy. We assumed that this three-dimensional structures were the same that (or similar to) bioactive conformation of the investigated compounds. All molecular modeling calculations (geometry optimization and conformational analysis) were performed using Gaussian03 software. 2D-QSAR study was done using Molecular Operating Environment software (MOE) (22, 23). The molecular structures of new analogues of FPh are presented in Scheme 1.

RESULTS AND DISCUSSION

Synthesis of the compounds

The new compounds **3–11** and **12** were synthesized as illustrated in Scheme 1. In the case of compounds **3–11**, the key intermediate was 10-(2,3-epoxypropyl)-2-trifluoromethyl-phenothiazine **2**. It was prepared *via* the treatment of commercially available 2-trifluoromethylphenothiazine **1** with 1-bromo-2,3-epoxypropane at room temperature in the presence of sodium hydride. The products **3–11** were obtained in the oxirane ring opening reaction of epoxide **2** with the appropriate amines. In contradistinction to remaining compounds, product **12** was prepared in one-step reaction of alkylation of initial phenothiazine **1** by means of 8-(2-pyrimidinyl)-8-aza-5-azaspiro[4,5]decane bromide. From the post reaction mixtures, the expected phenothiazines **3–11** and **12** were separated by column chro-

matography or crystallization. The yield of reactions was in the range of 10–55%. No effort was made to optimize the reaction conditions to increase the yields. It is known that during the synthesis, as shown in Scheme 1, secondary reactions such as polymerization and condensation diminish the yield (24). For pharmacological purposes the obtaining free bases of compounds **3–11** and **12** were converted to the corresponding water soluble hydrochlorides.

Biological activity

In vitro pro-apoptotic activity and pro-necrotic effect (cytotoxicity) of newly synthesized analogues of FPh were carried out in cultures of human lymphocytes genotoxicity damaged by incubation with B[a]P (7.5 μ M, 48 h). Results revealed that tested analogues of FPh differed markedly in their pro-apoptotic activity and pro-necrotic effect. It was noticed that compounds **3**, **4**, **6–9** and **12** exerted a pro-apoptotic effect markedly stronger than that of fluphenazine, and compounds **3**, **9** and **10** exhibited the weakest influence on frequency of necrotic lymphocyte in cultures (Table 1). The A/N ratios calculated for compounds **5**, **10** and **11** were lower by 10–15 times in comparison to the parent compound (FPh), whereas those calculated for compounds **3**, **9** and **12** were 3–7.5 times higher as that calculated for FPh (Table 1).

2D-QSAR study

In the classical 2D-QSAR investigation the database is divided into a training and a test set.

Table 1. Experimental values of ED₅₀ and TD₅₀, and calculated pED₅₀, pTD₅₀ and A/N index.

COMPOUND	ED ₅₀ [μ M]	pED ₅₀	TD ₅₀ [μ M]	pTD ₅₀	A/N index
3	7.33	5.13	46.88	4.33	3.24
4	6.00	5.22	29.41	4.53	2.47
5	14.3	4.84	14.89	4.83	0.53
6	6.70	5.17	25.87	4.59	1.95
7	7.46	5.13	46.37	4.33	3.15
8	8.17	5.09	32.02	4.49	1.98
9	7.40	5.13	44.66	4.35	3.05
10	19.5	4.71	11.02	4.96	0.28
11	10.33	4.99	13.91	4.86	0.68
12	6.98	5.16	102.85	3.99	7.44
FPh	8.58	5.07	16.97	4.77	1.0

pED₅₀ = $\log [1/(ED_{50} \times 10^6)]$; pTD₅₀ = $\log [1/(TD_{50} \times 10^6)]$; A/N index: the results (ED₅₀/TD₅₀) obtained in cultures with the tested compound compared to reference cultures (FPh = 1.0)

Table 2. Symbols for the QSAR descriptors and their definition.

Code of descriptor	Description
chl_C	Carbon connectivity index (order 1). This is calculated as the sum of $1/\sqrt{d_i d_j}$ over all bonds between carbon atoms i and j where $i < j$.
E_sol	Solvation energy. In the Potential Setup panel, the term enable flag is ignored, but the term weight is applied.
GCUT_PEOE_1	The GCUT descriptors are calculated from the eigenvalues of a modified graph distance adjacency matrix. Each ij entry of the adjacency matrix takes the value $1/\sqrt{d_{ij}}$ where d_{ij} is the (modified) graph distance between atoms i and j . The diagonal takes the value of the PEOE partial charges. The resulting eigenvalues are sorted and the smallest, 1/3-ile, 2/3-ile and largest eigenvalues are reported.
dipoleX	The x component of the dipole moment (external coordinates).
E_stb	Bond stretch-bend cross-term potential energy. In the Potential Setup panel, the term enable flag is ignored, but the term weight is applied.
a_hyd	Number of hydrophobic atoms.
DASA	Absolute value of the difference between ASA+ and ASA- where ASA+ -water accessible surface area of all atoms with positive partial charge (strictly greater than 0) and ASA- water accessible surface area of all atoms with negative partial charge (strictly less than 0).
PEOE_VSA_4	Sum of v_i where q_i is in the range (-0.25,-0.20). (PARTIAL CHARGE DESCRIPTOR)
SlogP	Log of the octanol/water partition coefficient (including implicit hydrogens). This property is an atomic contribution model that calculates logP from the given structure; i.e., the correct protonation state (washed structures). Results may vary from the logP(o/w) descriptor. The training set for SlogP was ~7000 structures.
PEOE_VSA_POL	Total polar van der Waals surface area. This is the sum of the v_i such that $ q_i $ is greater than 0.2. The v_i are calculated using a connection table approximation.
E_oop	Out-of-plane potential energy. In the Potential Setup panel, the term enable flag is ignored, but the term weight is applied.
E_vdw	van der Waals component of the potential energy. In the Potential Setup panel, the term enable flag is ignored, but the term weight is applied.

Because we had only 10 compounds we resign from this division. To perform quantitative structure-activity relationship study we calculated molecular descriptors for all compounds in database. Molecular descriptors are transformed into numbers - different chemical information (physicochemical properties) contained in the molecule. MOE program can calculate over 600 molecular descriptors including topological indices, structural keys, E-state indices, physical properties (such as log of the octanol/water partition coefficient, molecular weight and molar refractivity), topological polar surface area (TPSA) and CCG's VSA descriptors with applicability to both biological activity and ADME property prediction (ADME - absorption, distribution, metabolism, and excretion). Table 2 defines the QSAR descriptors used in our work.

The consecutive steps were: calculation, selection and evaluation of chemical structure descriptors for each compound in the database. Molecular descriptors were obtained with the QuaSAR-descriptor panel implemented in MOE molecular modeling

software. Descriptors with constant and near-constant values (the same or almost the same value for each compound in the training set) were eliminated. Also descriptors that are highly degenerate (strong interrelationship between descriptors) and those that showed very low correlation with biological activity ($r^2 < 0.2$) were reduced. To find correlation between molecular structure of the new synthesized analogues of FPh and its physicochemical properties (which were expressed by molecular descriptors) we used PLS (Partial Least Squares) statistical method. The final result of this investigation was to generate a few 2D-QSAR models. Next steps, like: validation, cross-validation (LOO: leave-one-out procedure) of the models, detection of outliers and modification of the QSAR models were used to improve the statistical power of the obtained QSAR equations. Compounds that "do not fit" into the equation (the greatest standard deviation), so-called outliers, were eliminated and not included in the formed models. If it was necessary and/or possible, also a number of descriptors was reduced in individual equations. It is

a very popular and effective method to improve the statistical quality of QSAR models. To build QSAR models, therefore, were not used every time all structures. A lack of the values of expected biological activity: pED_{50} pTD_{50} in Tables 3 and 4 for certain compounds indicates that these structures weren't used to the building of the respective models (there were so-called outliers).

Interpretation of the 2D-QSAR models was the last step, which is presented in the next chapter. In order to select suitable (proper) descriptors that could affect the biological activity of the investigated compounds, correlation analysis was performed. PLS statistical method was used to establish the 2D-QSAR models. Below, we provide a few QSAR equations which were generated from both neutral and protonated forms of FPh analogues, and a pro-apoptotic activity and a pro-necrotic effect, were used as a measure of biological activity of tested compounds.

In the case of pro-apoptotic activity of compounds as dependent and descriptors as independent value we obtained following 2D-QSAR equations: Model 1 and Model 2 for neutral forms of investigated compounds:

Model 1: $pED_{50} = 5.89554 - 0.10098 \times \text{chil_C} - 0.00220 \times E_{\text{sol}}$; $R^2 = 0.91$; $XR^2 = 0.86$; $RMSE = 0.04$; $XRMSE = 0.05$.

Model 2: $pED_{50} = 6.94063 - 0.05506 \times a_{\text{hyd}} + 1.43680 \times \text{GCUT_PEOE_1}$; $R^2 = 0.97$; $XR^2 = 0.90$; $RMSE = 0.03$; $XRMSE = 0.05$.

Model 3, 4 and 5 for monoprotonated forms:

Model 3: $pED_{50} = 5.29996 - 0.11336 \times \text{dipoleX} - 0.14243 \times E_{\text{stb}}$; $R^2 = 0.91$; $XR^2 = 0.75$; $RMSE = 0.08$; $XRMSE = 0.05$.

Model 4: $pED_{50} = 4.88967 + 0.00117 \times \text{DASA} - 0.11526 \times \text{dipoleX}$; $R^2 = 0.91$; $XR^2 = 0.78$; $RMSE = 0.07$; $XRMSE = 0.04$.

Model 5: $pED_{50} = 4.95715 - 0.11096 \times \text{dipoleX} + 0.01803 \times \text{PEOE_VSA_4}$; $R^2 = 0.94$; $XR^2 = 0.74$; $RMSE = 0.08$; $XRMSE = 0.04$.

In the above models adequacy was measured as the square of correlation coefficient (R^2), root mean square error (RMSE), cross-validated R^2 (XR^2) and cross-validated RMSE (XRMSE). The predictive power of the obtained models was expressed by statistical parameters: R^2 and XR^2 values, which should be close to one and resemble each other. The best models were obtained for neutral form. Equation 2 with the highest correlation coefficient (0.97) and cross-validated correlation coefficient XR^2 (0.90) seems to be the best model. This

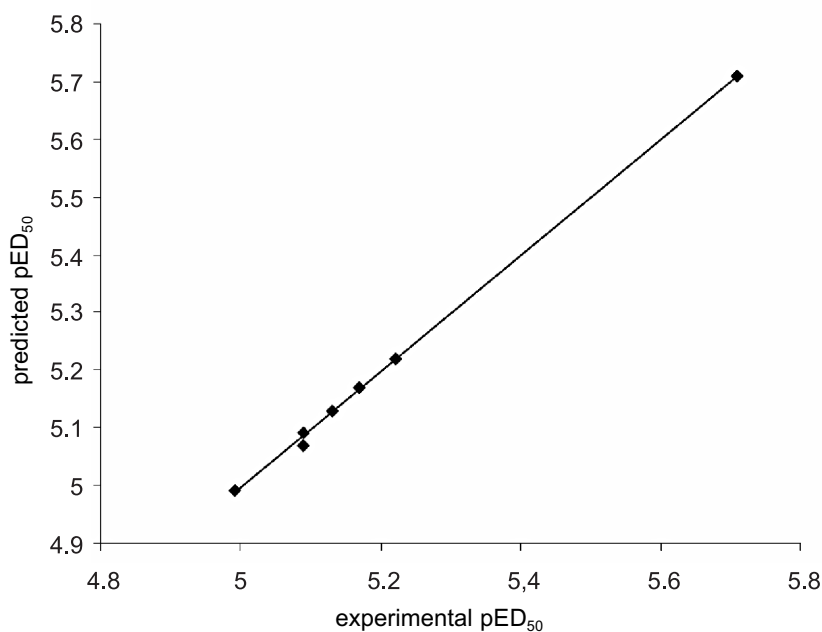


Figure 1. Plot of predicted pED_{50} against observed values for QSAR model by Equation 2

Table 3. Experimental pED₅₀ and predicted pED₅₀ values for investigated compounds.

Compound	Experimental pED ₅₀	Predicted pED ₅₀				
		Model 1	Model 2	Model 3	Model 4	Model 5
3	5.13	5.17	5.13	5.08	5.11	5.10
4	5.22	5.12	5.22	5.23	5.19	5.17
5	4.84	—	—	4.85	4.87	4.82
6	5.17	5.18	5.17	5.15	5.10	5.12
7	5.13	5.14	5.13	5.07	5.15	5.12
8	5.09	5.11	5.09	5.19	5.10	5.15
9	5.13	5.10	—	—	—	—
10	4.71	4.71	4.71	4.73	4.70	4.72
11	4.99	5.01	4.99	—	—	—
12	5.16	5.15	—	5.11	5.12	5.16
FPh	5.09	5.11	5.07	5.11	5.17	5.14

Table 4. Experimental pTD₅₀ and predicted pTD₅₀ values for investigated compounds.

Compound	Experimental pTD ₅₀	Predicted pTD ₅₀		
		Model 1	Model 2	Model 3
3	4.33	4.33	4.26	4.49
4	4.53	4.55	4.55	4.47
5	4.83	—	—	4.63
6	4.59	4.54	4.62	a.52
7	4.33	4.40	4.41	4.63
8	4.49	4.61	4.51	4.50
9	4.35	—	—	—
10	4.96	5.00	4.98	4.98
11	4.86	4.84	4.84	—
12	3.99	—	—	3.99
FPh	4.77	4.60	4.69	4.62

model correlate pED₅₀ value with two molecular descriptors: a_{hyd} and GCUT_PEOE_1. Only first parameter has clear structural interpretation, physico-chemical meaning - it reflects a number of hydrophobic atoms in a tested compound. This descriptor is negatively correlated with pED₅₀ value so increasing their value will lead to a decrease of pED₅₀ (reduced pro-apoptotic activity of the investigated compounds). Models 3, 4 and 5 show correlation coefficients about 0.9 (very high) but their cross-validated correlation coefficients is smaller than in models 1 and 2. In this three models the same descriptor appears - dipoleX. This is an x component of the dipole moment. It can be suggested that

reducing this parameter may increase biological activity. The predictive power of obtained models experimental and predicted pro-apoptotic activity were listed in Table 3 and showed in Figure 1.

In the case of a pro-necrotic effect of compounds as dependent- and descriptors as independent value we obtained the following 2D-QSAR equations:

Model 1 and Model 2 for neutral forms of investigated compounds:

Model 1: pTD₅₀ = 3.72121 + 0.2042 × SlogP; R² = 0.86; XR² = 0.81; RMSE = 0.10; XRMSE = 0.08.

Model 2: pTD₅₀ = 4.04217 + 0.17981 × SlogP –

$0.00515 \times \text{PEOE_VSA_POL}$; $R^2 = 0.95$; $\text{XR}^2 = 0.87$; $\text{RMSE} = 0.05$; $\text{XRMSE} = 0.08$

Monoprotonated forms of the investigated compounds:

Model 3: $\text{pTD}_{50} = 3.54723 - 0.06107 \times \text{E}_{\text{oop}} + 0.01836 \times \text{E}_{\text{vdw}}$; $R^2 = 0.95$; $\text{XR}^2 = 0.87$
 $\text{RMSE} = 0.14$; $\text{XRMSE} = 0.17$.

In models 1 and 2 we applied a descriptor – SlogP - that was log of the octanol/water partition coefficient. This parameter is very important especially for bioactive compounds – drugs which should overpass biological lipid membranes (for example blood-brain barrier). The above QSAR equations suggest that increasing this value may increase the biological activity. Also other two descriptors: PEOE_VSA_POL and E_{oop} play an important role in pro-necrotic effect (cytotoxicity) of new synthesized analogues of FPh – but are negatively correlated with pTD₅₀.

Experimental pTD₅₀ and predicted pTD₅₀ values for tested compounds are presented in Table 4.

CONCLUSION

2D-QSAR equations, described in this publication, indicate the relationship between biological activity and the corresponding descriptors. Table 2 presents abbreviations, full names and description of all the descriptors used in the final 2D-QSAR models. Some of them have quite clear physical meaning, but unfortunately, most of them is often “a combination of” a few physical and chemical properties. Rarely happens that the biological activity of the drug is dependent on one or a few obvious and clear properties. Many factors have an influence on the biological activity of the compound and getting to know them isn't easy. Time-consuming and costly researches of specialists in the drug design confirm this facts. Obtained 2D-QSAR models allow to predict the activity of a new compound on the basis of its structure without the need of its synthesis. Estimate of the expected (predicted) biological activity for the next analog can be made by optimizing the geometry of the compound in a suitable computer program and using appropriate computational quantum chemistry methods and then compute the so-called molecular descriptors. Then, the obtained values of descriptors are substituted for the found earlier, reliable 2D-QSAR models and used to calculate a predicted value for the biological activity of a new derivative of the analyzed group of compounds. In

order to propose structural modifications that can be taken into account in the further synthesis of next analogues, we plan to carry out a three-dimensional QSAR analysis (COMFA and CoMSIA). It involves the generation, for a series of compounds, so-called molecular field, which allows to visual identification of areas with positive or negative impact on the biological activity (spatial maps of steric and electrostatic interactions). This will be the next step in the study of the relationship between the pro-apoptotic activity and the structure of new analogues of FPh.

We found the obtained QSAR models suitable for predicting the activity of new synthesized FPh analogues. On the basis of QSAR equations we shall be able to propose new structures of Pht, which should exert a strong pro-apoptotic activity and a weak pro-necrotic effect on genotoxicity-damaged cells and cancer cells.

REFERENCES

1. Claxton K.L., Chen J.J., Swope D.M.: *J. Pharm. Pract.* 20, 415 (2007).
2. Jaszczyszyn A., Gąsiorowski K., Świątek P., Malinka W., Cieślak-Boczula K., Petrus J., Czarnik-Matusewicz B.: *Pharmacol. Rep.* 64, 16 (2012).
3. Jaszczyszyn A., Gąsiorowski K., Świątek P., Malinka W., Cieślak-Boczula K., Petrus J., Czarnik-Matusewicz B.: *Współcz. Onkol.* 16, 332 (2012).
4. Bisi A., Meli M., Gobbi S., Tolomeo M., Dusonchet L.: *Bioorg. Med. Chem.* 16, 6474 (2008).
5. Morak-Młodawska B., Jeleń M., Pluta K.: *Pol. Merkuriusz Lek.* 26, 671 (2009).
6. Catts V.S., Catts S.V., O'Toole B.I., Frost A.D.: *Acta Psychiatr. Scand.* 117, 323 (2008).
7. Gil-Ad I., Shtaf B., Levkovitz Y., Nordenberg J., Taler M., Korov I., Weizman A.: *Oncol. Rep.* 15, 107 (2006).
8. Choi J.H., Yang Y.R., Lee S.K., Kim S.H., Kim Y.H., Cha J.Y., Oh S.W., Ha J.R., Ryu S.H., Suh P.G.: *Ann. N. Y. Acad. Sci.* 1138, 393 (2008).
9. Sun S.Y., Hail N., Lotan R.: *J. Natl. Cancer Inst.* 96, 662 (2004).
10. Jaszczyszyn A., Gąsiorowski K., Świątek P., Malinka W.: *Onkol. Pol.* 12, 143 (2009).
11. Gąsiorowski K., Jaszczyszyn A.: *Onkol. Pol.* 11, 147 (2008).
12. Jaszczyszyn A., Gąsiorowski K., Świątek P., Malinka W.: *Onkol. Pol.* 14, 43 (2011).

13. Levinson D.F., Simpson G.M., Lo E.S., Cooper T.B., Singh H., Yadalam K., Stephanos M.J.: *Am. J. Psychiatry* 152, 765 (1995).
14. Jaszczyszyn A., Gąsiorowski K.: *Chemopreventive mechanisms of action of newly synthesized analogs of fluphenazine (Polish) Borgis®* Wydawnictwo Medyczne, Warszawa 2006.
15. Frisch M.J., Trucks G.W., Schlegel H.B., Scuseria G.E., Robb M.A., Cheeseman J.R., Montgomery Jr J.A., Vreven T., Kudin K.N., Burant J.C., Millam J.M., Iyengar S.S., Tomasi J., Barone V., Mennucci B., Cossi M., Scalmani G., Rega N., Petersson G.A., Nakatsuji H., Hada M., Ehara M., Toyota K., Fukuda R., Hasegawa J., Ishida M., Nakajima T., Honda Y., Kitao O., Nakai H., Klene M., Li X., Knox J.E., Hratchian H.P., Cross J.B., Adamo C., Jaramillo J., Gomperts R., Stratmann R.E., Yazyev O., Austin A.J., Cammi R., Pomelli C., Ochterski J.W., Ayala P.Y., Morokuma K., Voth G.A., Salvador P., Dannenberg J.J., Zakrzewski V.G., Dapprich S., Daniels A.D., Strain M.C., Farkas O., Malick D.K., Rabuck A.D., Raghavachari K., Foresman J.B., Ortiz J.V., Cui Q., Baboul A.G., Clifford S., Cioslowski J., Stefanov B.B., Liu G., Liashenko A., Piskorz P., Komaromi I., Martin R.L., Fox D.J., Keith T., Al-Laham M.A., Peng C.Y., Nanayakkara A., Challacombe M., Gill P.M.W., Johnson B., Chen W., Wong W., Gonzalez C., Pople J.A.: *Gaussian 03, Revision C.02*, Gaussian, Inc., Wallingford CT 2004.
16. Tsakovska I.M.: *Bioorg. Med. Chem.* 11, 2889 (2003).
17. McDowell J.J.H.: *Acta. Cryst. B* 36, 2178 (1980).
18. Pajeva I.K., Wiese M.: *J. Med. Chem.* 45, 5671 (2002).
19. Pajeva I.K., Globisch C., Wiese M.: *J. Med. Chem.* 47, 2523 (2004).
20. Pajeva I.K., Wiese M.: *J. Med. Chem.* 41, 1815 (1998).
21. Tsakovska I., Pajeva I.: *Curr. Drug Targets* 7, 1123 (2006).
22. MOE, Molecular Operating Environment, 2005.06; Chemical Computing Group Inc.: Montreal 2005.
23. Systat 11, 12 software (Systat Software, Inc.).
24. Leuschner J., Schafer H., Leuschner F.: *Eur. J. Med. Chem.* 29, 241 (1994).

Received: 18. 10. 2012